

Supplementary material

Catalytic Dioxygenation of Flavonol by M^{II} -Complexes ($M = Mn, Fe, Co, Ni, Cu$ and Zn)----Mimicking the M^{II} - Substituted Quercetin 2,3-Dioxygenase

Table of Contents

X-ray Structure Determinations.

Table Caption

Table S1. Summary of X-ray data collection and refinement for the complex $[(\text{Fe}^{\text{III}}\text{L})_2(\mu\text{-O})(\mu\text{-OAc})]\text{Cl}\cdot 10\text{H}_2\text{O}$ (**2B**).

Table S2. Selected bond distances (Å) and bond angles (°) for the complex $[(\text{Fe}^{\text{III}}\text{L})_2(\mu\text{-O})(\mu\text{-OAc})]\text{Cl}\cdot 10\text{H}_2\text{O}$ (**2B**).

Table S3. The solution FT-IR results of the complexes $[\text{M}^{\text{II}}\text{L}(\text{OAc})]$ in ethanol.

Table S4. The products analysis results of the dioxygenation of flavonol catalyzed by the complexes $[\text{M}^{\text{II}}\text{L}(\text{OAc})]$ in DMF.

Table S5. Kinetic data for the dioxygenation of flavonol catalyzed by the complexes $[\text{M}^{\text{II}}\text{L}(\text{OAc})]$ and $[(\text{Fe}^{\text{III}}\text{L})_2(\mu\text{-O})(\mu\text{-OAc})]\text{Cl}$ (**2B**) in DMF.

Figure Caption

Figure S1. ESI-MS spectrum of the complexes. Insert: The molecular peak cluster of $[\text{M}^{\text{II}}\text{L}(\text{OAc})]\text{H}^+$ (M: Mn, Co, Ni, Cu) or $[\text{Fe}^{\text{III}}\text{L}(\text{OAc})]^+$ (Line: experiment, column: calculated). (a) $[\text{Mn}^{\text{II}}\text{L}(\text{OAc})]$ (**1**), (b) $[\text{Fe}^{\text{II}}\text{L}(\text{OAc})]$ (**2**), (c) $[\text{Co}^{\text{II}}\text{L}(\text{OAc})]$ (**3**), (d) $[\text{Ni}^{\text{II}}\text{L}(\text{OAc})]$ (**4**), (e) $[\text{Cu}^{\text{II}}\text{L}(\text{OAc})]$ (**5**), (f) $[\text{Zn}^{\text{II}}\text{L}(\text{OAc})]$ (**6**).

Figure S2. The FT-IR spectra of the ethanol solution and solid sample of $[\text{Ni}^{\text{II}}\text{L}(\text{OAc})]$ (**4**). (A) solvent ethanol, (B) solid sample of $[\text{Ni}^{\text{II}}\text{L}(\text{OAc})]$, (C) ethanol solution of $[\text{Ni}^{\text{II}}\text{L}(\text{OAc})]$.

Figure S3. The EPR spectra of $[\text{Co}^{\text{II}}\text{L}(\text{OAc})]$ (**3**) (4 mM in 0.5 mL DMF) at 100 K. A: under N_2 , B: in the presence of 1 eq. flaH under N_2 .

Figure S4. Cyclic voltammograms of (a) $[\text{Fe}^{\text{II}}\text{L}(\text{OAc})]$ (**2**), (b) $[\text{Co}^{\text{II}}\text{L}(\text{OAc})]$ (**3**), (c) $[\text{Cu}^{\text{II}}\text{L}(\text{OAc})]$ (**5**) and flavonol in the presence of 1 eq. (d) $[\text{Mn}^{\text{II}}\text{L}(\text{OAc})]$ (**1**), (e) $[\text{Co}^{\text{II}}\text{L}(\text{OAc})]$ (**3**), (f) $[\text{Ni}^{\text{II}}\text{L}(\text{OAc})]$ (**4**), (g) $[\text{Cu}^{\text{II}}\text{L}(\text{OAc})]$ (**5**) and (h) $[\text{Zn}^{\text{II}}\text{L}(\text{OAc})]$ (**6**) in DMF.

Figure S5. The HPLC-MS spectra of the reaction products of dioxygenation of flavonol catalyzed by $[\text{Co}^{\text{II}}\text{L}(\text{OAc})]$ (**3**) at 70 °C for 12 hrs. (a) HPLC spectra. MS spectra of (b) HObs m/z (pos.): 260.1 ($\text{M} + \text{NH}_4$)⁺, (c) benzoic acid m/z (neg.): 121.3 ($\text{M} - \text{H}$)⁻, 181.1 ($\text{M} + \text{CH}_3\text{COO}$)⁻, (d) salicylic acid m/z (neg.): 137.2 ($\text{M} - \text{H}$)⁻, (e) *N,N*-dimethylbenzamide m/z (pos.): 150.2 ($\text{M} + \text{H}$)⁺ and (f) 2-hydroxy-*N,N*-dimethylbenzamide m/z (pos.): 166.2 ($\text{M} + \text{H}$)⁺.

Figure S6. Detection of the production of CO during dioxygenation reaction of flavonol catalyzed by $[\text{Co}^{\text{II}}\text{L}(\text{OAc})]$ (**3**) at 70 °C. (a) Plot of the CO concentration vs. reaction time. (b) Plot of the integrated CO concentration vs. reaction time.

Figure S7. ¹H NMR spectra of two main products of reaction of flavonol (2.5×10^{-2} M in 200 mL DMF) with O_2 catalyzed by $[\text{Co}^{\text{II}}\text{L}(\text{OAc})]$ (**3**) (5% mol) at 100 °C for 7 days after esterification by CH_3OH in the presence of H_2SO_4 at ambient temperature. (a) salicylic acid methyl ester (b) benzoic acid methyl ester.

Figure S8. Eyring plot for the dioxygenation of flavonol catalyzed by the complexes $[\text{M}^{\text{II}}\text{L}(\text{OAc})]$ in DMF.

Figure S9. Spectral changes accompanying the titration of the complex (a) **2B**, (c) **1**, (d) **2**, (e) **3**, (f) **4**, (g) **5** and (h) **6**

(1.0×10^{-4} M except **2B** 0.5×10^{-4} M) by flavonol under N_2 . Inset: Absorbance changes at λ_{\max} vs. eq. of flaH, (b) ESI-MS spectrum of the titration solution of **2B**.

Figure S10. The UV-vis spectra of the complexes $[M^{II}L(OAc)]$ (0.1 mM) (red) and in the presence of equivalent amount of flavonol (black) (a) $[Mn^{II}L(OAc)]$ (**1**), (b) $[Fe^{II}L(OAc)]$ (**2**), (c) $[Co^{II}L(OAc)]$ (**3**), (d) $[Ni^{II}L(OAc)]$ (**4**), (e) $[Cu^{II}L(OAc)]$ (**5**), (f) $[Zn^{II}L(OAc)]$ (**6**) (g) ESI-MS spectrum of the solution of $[Co^{II}L(OAc)] + 1$ eq. flaH after exposure to O_2 . Inset: The peak cluster of $[M^{II}L(flac)]H^+$ (M: Mn, Ni, Cu) or $[M^{III}L(flac)]^+$ (M: Fe, Co) (Line: experiment, column: calculated).

X-ray Structure Determinations

Intensity data were measured at 293(2) K on a Bruker SMART APEX II CCD area detector system. Data reduction and unit cell refinement were performed with Smart-CCD software [1]. The structures were solved by direct methods using SHELXS-97 and were refined by full-matrix least squares methods using SHELXL-97. [2]

For **2A**, all non-hydrogen atoms were refined anisotropically. The hydrogen atoms related to carbon atoms were generated geometrically. Since the disordered H₂O solvent molecules could not be unambiguously modeled, the Platon Squeeze option was utilized to process the data.[3] Squeeze indicates 2 solvent regions in the cell corresponding to about 94 electrons/cell or approximately 4.5 H₂O molecules per formula.

For **2B**, all non-hydrogen atoms were refined anisotropically. The hydrogen atoms related to carbon atoms were generated geometrically. “DELU” limits were used for two C atoms from the ligands. Since the disordered H₂O solvent molecules could not be unambiguously modeled, the Platon Squeeze option was utilized to process the data.[3] Squeeze indicates 8 solvent regions in the cell corresponding to about 788 electrons/cell or approximately 10 H₂O molecules per formula.

For **3A**, all non-hydrogen atoms were refined anisotropically. The hydrogen atoms related to carbon atoms were generated geometrically. Since the disordered H₂O solvent molecules could not be unambiguously modeled, the Platon Squeeze option was utilized to process the data.[3] Squeeze indicates 2 solvent regions in the cell corresponding to about 84 electrons/cell or approximately 4 H₂O molecules per formula.

For **4A**, all non-hydrogen atoms were refined anisotropically. The hydrogen atoms related to carbon atoms were generated geometrically. The hydrogen atom attached to coordinated MeOH was located from the difference Fourier map and refined with restrained O-H distance. Since the disordered H₂O solvent molecules could not be unambiguously modeled, the Platon Squeeze option was utilized to process the data.[3] Squeeze indicates 4 solvent regions in the cell corresponding to about 68 electrons/cell or approximately 3.5 H₂O molecules per formula.

For **5**, all non-hydrogen atoms were refined anisotropically. The hydrogen atoms related to carbon atoms were generated geometrically. All hydrogen atoms attached to oxygen atoms were located from the difference Fourier map and refined with restrained O-H and H···H distances.

Reference:

[1] *XSCANS* (Version 2.1), Siemens Analytical X-Ray Instruments Inc., Madison, WI, **1994**.

[2] G. M. Sheldrick, *SHELXL-97, Program for X-ray Crystal Structure Refinement*, University of Göttingen: Göttingen, (Germany), **1997**.

[3] SQUEEZE (handling of disordered solvents in structure refinement). A. L. Spek. *J. Appl. Crystallogr.* 2003, **36**, 7.

Table S1. Summary of X-ray data collection and refinement for the complex [(Fe^{III}L)₂(μ-O)(μ-OAc)]Cl·10H₂O (**2B**).

empirical formula	C ₄₄ H ₄₃ ClFe ₂ N ₆ O ₉	crystal habit	block
<i>M_r</i>	946.99	Crystal color	brown
crystal system	tetragonal	crystal size (mm ³)	0.20 × 0.15 × 0.10
space group	<i>I4(1)cd</i>	<i>μ</i> /mm ⁻¹	0.684
<i>a</i> /Å	16.545(5)	2 <i>θ</i> _{max} /deg	50.00
<i>b</i> /Å	16.545(5)	completeness to <i>θ</i> (%)	99.6
<i>c</i> /Å	36.72(2)	reflections collected	26254
<i>α</i> /deg	90	independent reflections	4245
<i>β</i> /deg	90	<i>R</i> _{int}	0.0733
<i>γ</i> /deg	90	<i>R</i> 1 ^a / <i>wR</i> 2 ^b [<i>I</i> >2 <i>σ</i> (<i>I</i>)]	0.0757/0.1976
<i>V</i> /Å ³	10052(8)	<i>R</i> 1 ^a / <i>wR</i> 2 ^b (all data)	0.1036/0.2150
<i>Z</i>	8	goodness-of-fit (<i>F</i> ²)	0.995
<i>D_x</i> / g cm ⁻³	1.251		
<i>T</i> /K	296(2)		

^a $R1 = \sum || F_o| - |F_c|| / \sum |F_o|$. ^b $wR2 = [\sum w (F_o^2 - F_c^2)^2 / \sum w(F_o^2)^2]^{1/2}$

Table S2. Selected bond distances (Å) and bond angles (°) for the complex [(Fe^{III}L)₂(μ-O)(μ-OAc)]Cl·10H₂O (**2B**).

bond distances (Å)		bond angles (°)	
Fe-N(1)	2.303(6)	O(1)-Fe-O(5)	103.12(16)
Fe-N(2)	2.122(8)	O(1)-Fe-O(4)	94.6(2)
Fe-N(3)	2.177(6)	O(1)-Fe-N(1)	87.2(2)
Fe-O(1)	1.985(5)	O(1)-Fe-N(2)	87.3(3)
Fe-O(4)	2.039(7)	O(1)-Fe-N(3)	159.9(2)
Fe-O(5)	1.804(3)	O(5)-Fe-N(1)	167.81(18)
		O(5)-Fe-N(2)	96.8(3)
		O(5)-Fe-N(3)	96.94(18)
		O(5)-Fe-O(4)	98.5(3)
		O(4)-Fe-N(1)	87.0(2)
		O(4)-Fe-N(2)	163.7(3)
		O(4)-Fe-N(3)	83.9(3)
		N(1)-Fe-N(2)	76.9(3)
		N(1)-Fe-N(3)	72.7(2)
		N(2)-Fe-N(3)	88.8(3)

Table S3. The solution FT-IR results of the complexes [M^{II}L(OAc)] in ethanol.

	[Mn ^{II} L(OAc)]	[Fe ^{II} L(OAc)]	[Co ^{II} L(OAc)]	[Ni ^{II} L(OAc)]	[Cu ^{II} L(OAc)]	[Zn ^{II} L(OAc)]
	(1)	(2)	(3)	(4)	(5)	(6)
COO ⁻ of L ⁻ :						
$\nu_{\text{as}}(\text{CO}_2)$ (cm ⁻¹)	1594	1594	1600	1605	1609	1605
$\nu_{\text{s}}(\text{CO}_2)$ (cm ⁻¹)	1413	1394	1405	1417	1409	1391
$\Delta\nu$ (cm ⁻¹)	181	200	195	188	200	214
OAc ⁻ :						
$\nu_{\text{as}}(\text{CO}_2)$ (cm ⁻¹)	1557	1557	1549	1558	1576	1583
$\nu_{\text{s}}(\text{CO}_2)$ (cm ⁻¹)	1413	1413	1402	1402	1379	1440
$\Delta\nu$ (cm ⁻¹)	144	144	147	156	197	143

Table S4. The products analysis results of the dioxygenation of flavonol catalyzed by the complexes [M^{II}L(OAc)] (5 mol %) in DMF for 12 hrs.

Catalyst	T (°C)	HObs	Yield (%)				Conv (%)	TON	Conv. rate (h ⁻¹)
			Benzoic acid	Salicylic acid	<i>N,N</i> -dimethyl benzamide	2-Hydroxy- <i>N,N</i> - dimethyl benzamide			
[Mn ^{II} L(OAc)] (1)	100		82.4	81.3			82.4	16.5	1.37
[Fe ^{II} L(OAc)] (2)	70		67.2	56.0		8.4	67.2	13.4	1.12
[Co ^{II} L(OAc)] (3)	70	27.2	25.4	55.1	23.4		82.3	16.5	1.37
[Ni ^{II} L(OAc)] (4)	70	13.5	30.5	55.7	36.8	7.5	80.8	16.2	1.35
[Cu ^{II} L(OAc)] (5)	100		80.5	78.2			80.5	16.1	1.34
[Zn ^{II} L(OAc)] (6)	100	16.7	48.8	65.4	16.7	9.40	91.5	18.3	1.50

Table S5. Kinetic data for the dioxygenation of flavonol catalyzed by the complexes $[\text{M}^{\text{II}}\text{L}(\text{OAc})]$ and $[(\text{Fe}^{\text{III}}\text{L})_2(\mu\text{-O})(\mu\text{-OAc})]\text{Cl}$ (**2B**) in DMF.

$[\text{Mn}^{\text{II}}\text{L}(\text{OAc})]$ (1)							
Exp. No.	T (°C)	$[\text{O}_2]_0$ (10^{-3} M)	$[\text{flaH}]_0$ (10^{-4} M)	$[\text{Mn}^{\text{II}}\text{L}(\text{OAc})]_0$ (10^{-6} M)	ν_{in} (10^{-8} M s $^{-1}$)	k (10^4 M $^{-2}$ s $^{-1}$)	k (10^4 M $^{-2}$ s $^{-1}$)
1	100	3.18	1.02	1.00	0.58	1.79 ± 0.07	
2	100	3.18	0.99	2.00	1.00	1.59 ± 0.05	
3	100	3.18	0.97	3.00	1.45	1.57 ± 0.04	
4	100	3.18	1.00	4.00	2.04	1.60 ± 0.06	
							1.65 ± 0.12
5	100	3.96	1.00	3.00	1.91	1.61 ± 0.05	
6	100	4.75	1.00	3.00	2.37	1.66 ± 0.03	
7	100	3.18	0.79	3.00	1.22	1.62 ± 0.09	
8	100	3.18	1.32	3.00	2.19	1.74 ± 0.07	
9	85	3.63	0.99	1.00	0.33	0.92 ± 0.05	
10	90	3.49	1.01	1.00	0.39	1.11 ± 0.07	
11	95	3.33	1.00	1.00	0.47	1.41 ± 0.04	

$[\text{Fe}^{\text{II}}\text{L}(\text{OAc})]$ (2)							
Exp. No.	T (°C)	$[\text{O}_2]_0$ (10^{-3} M)	$[\text{flaH}]_0$ (10^{-4} M)	$[\text{Fe}^{\text{II}}\text{L}(\text{OAc})]_0$ (10^{-6} M)	ν_{in} (10^{-8} M s $^{-1}$)	k (10^4 M $^{-2}$ s $^{-1}$)	k (10^4 M $^{-2}$ s $^{-1}$)
1	70	4.02	0.89	1.00	0.21	0.58 ± 0.10	
2	70	4.02	0.89	2.00	0.40	0.55 ± 0.08	
3	70	4.02	0.91	3.00	0.62	0.56 ± 0.07	
4	70	4.02	0.89	4.00	0.80	0.56 ± 0.04	
							0.55 ± 0.02
5	70	4.87	0.90	3.00	0.72	0.55 ± 0.08	
6	70	5.72	0.89	3.00	0.81	0.53 ± 0.04	
7	70	4.02	0.65	3.00	0.45	0.57 ± 0.05	
8	70	4.02	1.10	3.00	0.69	0.52 ± 0.05	
9	75	3.90	0.87	3.00	0.84	0.83 ± 0.06	
10	90	3.49	0.87	3.00	1.13	1.24 ± 0.05	
11	95	3.33	0.89	3.00	1.42	1.60 ± 0.04	

[Co^{III}L(OAc)] (3)

Exp. No.	T (°C)	[O ₂] ₀ (10 ⁻³ M)	[flaH] ₀ (10 ⁻⁴ M)	[Co ^{III} L(OAc)] ₀ (10 ⁻⁶ M)	ν_{in} (10 ⁻⁷ M s ⁻¹)	k (10 ⁵ M ⁻² s ⁻¹)	k (10 ⁵ M ⁻² s ⁻¹)
1	70	4.02	1.05	2.00	4.94	5.85 ± 0.11	
2	70	4.02	1.05	1.50	3.64	5.75 ± 0.06	
3	70	4.02	1.07	1.00	2.49	5.79 ± 0.09	
4	70	4.02	1.03	0.50	1.17	5.65 ± 0.04	
5	70	4.02	0.90	0.50	1.06	5.86 ± 0.11	5.79 ± 0.08
6	70	4.02	1.32	0.50	1.55	5.84 ± 0.07	
7	55	5.23	0.96	1.00	1.59	3.17 ± 0.10	
8	55	6.12	0.94	1.00	1.96	3.40 ± 0.07	
9	55	4.34	0.95	1.00	1.39	3.38 ± 0.04	
10	60	4.24	1.05	1.00	1.83	4.11 ± 0.07	
11	65	4.13	1.08	1.00	2.16	4.84 ± 0.07	

[Ni^{III}L(OAc)] (4)

Exp. No.	T (°C)	[O ₂] ₀ (10 ⁻³ M)	[flaH] ₀ (10 ⁻⁴ M)	[Ni ^{III} L(OAc)] ₀ (10 ⁻⁶ M)	ν_{in} (10 ⁻⁸ M s ⁻¹)	k (10 ⁵ M ⁻² s ⁻¹)	k (10 ⁵ M ⁻² s ⁻¹)
1	70	4.02	1.03	2.00	8.36	1.00 ± 0.07	
2	70	4.02	1.02	1.50	5.67	0.92 ± 0.09	
3	70	4.02	1.07	1.00	4.11	0.98 ± 0.04	
4	70	4.02	0.96	0.50	1.69	0.88 ± 0.07	
5	70	4.02	0.82	1.00	3.10	0.94 ± 0.09	0.95 ± 0.07
6	70	4.02	1.34	1.00	5.84	1.08 ± 0.11	
7	70	4.87	1.05	1.00	4.77	0.93 ± 0.10	
8	70	5.72	1.05	1.00	5.33	0.88 ± 0.05	
9	75	3.90	1.01	1.00	4.45	1.13 ± 0.07	
10	80	3.79	1.00	1.00	5.23	1.38 ± 0.05	
11	90	3.49	1.04	1.00	7.26	2.00 ± 0.09	

[Cu^{II}L(OAc)] (5)

Exp. No.	T (°C)	[O ₂] ₀ (10 ⁻³ M)	[flaH] ₀ (10 ⁻⁴ M)	[Cu ^{II} L(OAc)] ₀ (10 ⁻⁶ M)	v_{in} (10 ⁻⁸ M s ⁻¹)	k (10 ⁴ M ⁻² s ⁻¹)	k (10 ⁴ M ⁻² s ⁻¹)
1	100	3.18	1.05	2.00	0.91	1.37 ± 0.07	
2	100	3.18	1.00	3.00	1.28	1.34 ± 0.11	
3	100	3.18	1.04	4.00	1.81	1.37 ± 0.09	
4	100	3.18	1.02	5.00	2.09	1.29 ± 0.05	
5	100	3.96	1.01	5.00	2.80	1.40 ± 0.11	1.35 ± 0.12
6	100	4.75	1.00	5.00	3.25	1.37 ± 0.12	
7	100	3.18	0.86	5.00	1.83	1.33 ± 0.11	
8	100	3.18	1.21	5.00	2.55	1.33 ± 0.09	
9	85	3.63	0.91	5.00	1.20	0.73 ± 0.08	
10	90	3.49	0.90	5.00	1.35	0.86 ± 0.11	
11	95	3.33	0.91	5.00	1.65	1.09 ± 0.07	

[Zn^{II}L(OAc)] (6)

Exp. No.	T (°C)	[O ₂] ₀ (10 ⁻³ M)	[flaH] ₀ (10 ⁻⁴ M)	[Zn ^{II} L(OAc)] ₀ (10 ⁻⁶ M)	v_{in} (10 ⁻⁸ M s ⁻¹)	k (10 ⁴ M ⁻² s ⁻¹)	k (10 ⁴ M ⁻² s ⁻¹)
1	100	3.18	0.80	2.00	2.26	4.44 ± 0.02	
2	100	3.18	0.80	3.00	3.30	4.45 ± 0.08	
3	100	3.18	0.79	4.00	4.38	4.40 ± 0.06	
4	100	3.18	0.72	5.00	5.47	4.78 ± 0.10	
5	100	3.18	0.90	5.00	6.30	4.40 ± 0.10	4.52 ± 0.03
6	100	3.96	0.89	5.00	7.80	4.43 ± 0.11	
7	100	4.75	0.87	5.00	9.89	4.78 ± 0.15	
8	100	3.18	0.27	5.00	1.97	4.58 ± 0.09	
9	100	3.18	0.55	5.00	4.13	4.56 ± 0.07	
10	100	3.18	0.65	5.00	4.58	4.43 ± 0.10	
11	100	3.18	0.93	5.00	6.27	4.24 ± 0.10	
12	85	3.63	0.80	5.00	3.73	2.57 ± 0.10	
13	90	3.49	0.80	5.00	4.20	3.01 ± 0.07	
14	95	3.33	0.80	5.00	4.92	3.69 ± 0.08	

$[(\text{Fe}^{\text{III}}\text{L})_2(\mu\text{-O})(\mu\text{-OAc})]\text{Cl}$ (2B)

Exp. No.	T (°C)	$[\text{O}_2]_0$ (10^{-3} M)	$[\text{flaH}]_0$ (10^{-4} M)	$[[(\text{Fe}^{\text{III}}\text{L})_2(\mu\text{-O})(\mu\text{-OAc})]\text{Cl}]_0$ (10^{-6} M)	v_{in} (10^{-9} M s $^{-1}$)
1	70	4.02	0.90	0.50	0.43
2	70	4.02	0.93	1.00	0.85
3	70	4.02	0.91	1.50	1.14
4	70	4.02	0.92	2.00	1.62
5	100	3.18	1.01	0.50	6.37
6	100	3.18	0.96	1.00	12.4
7	100	3.18	0.97	1.50	18.5
8	100	3.18	0.97	2.00	24.7

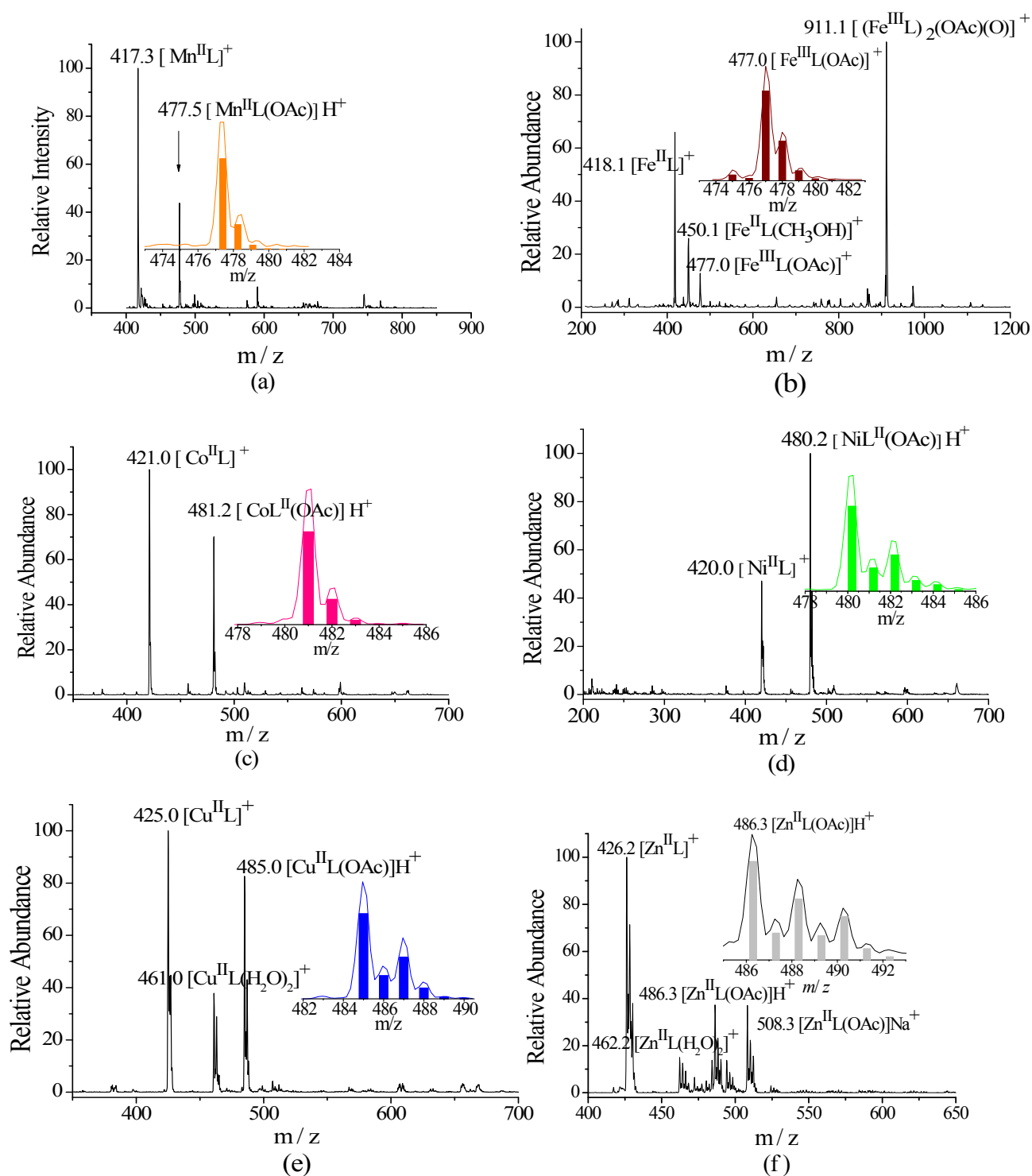


Figure S1. ESI-MS spectra of the complexes. Insert: The molecular peak cluster of $[M^{II}L(OAc)]H^+$ (M: Mn, Co, Ni, Cu) or $[Fe^{III}L(OAc)]^+$ (Line: experiment, column: calculated). (a) $[Mn^{II}L(OAc)]$ (**1**), (b) $[Fe^{III}L(OAc)]$ (**2**), (c) $[Co^{II}L(OAc)]$ (**3**), (d) $[Ni^{II}L(OAc)]$ (**4**), (e) $[Cu^{II}L(OAc)]$ (**5**), (f) $[Zn^{II}L(OAc)]$ (**6**).

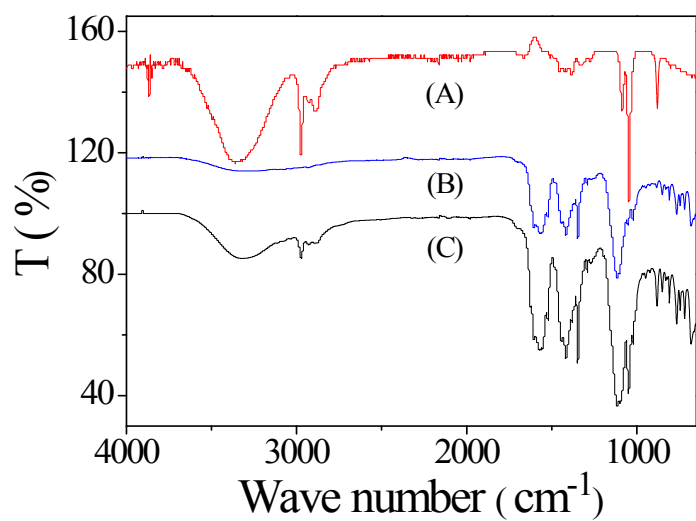


Figure S2. The FT-IR spectra of the ethanol solution and solid sample of $[\text{Ni}^{\text{II}}\text{L}(\text{OAc})]$ (**4**). (A) solvent ethanol (B) solid sample of $[\text{Ni}^{\text{II}}\text{L}(\text{OAc})]$ (C) ethanol solution of $[\text{Ni}^{\text{II}}\text{L}(\text{OAc})]$.

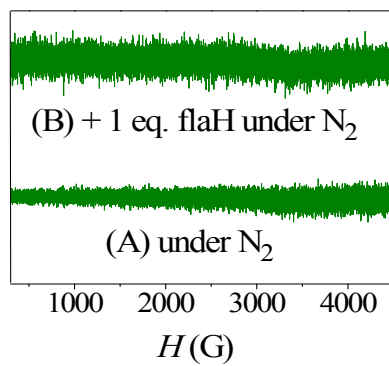


Figure S3. The EPR spectra of [Co^{II}L(OAc)] (**3**) (4 mM in 0.5 mL DMF) at 100 K. A: under N₂, B: in the presence of 1 eq. flaH under N₂.

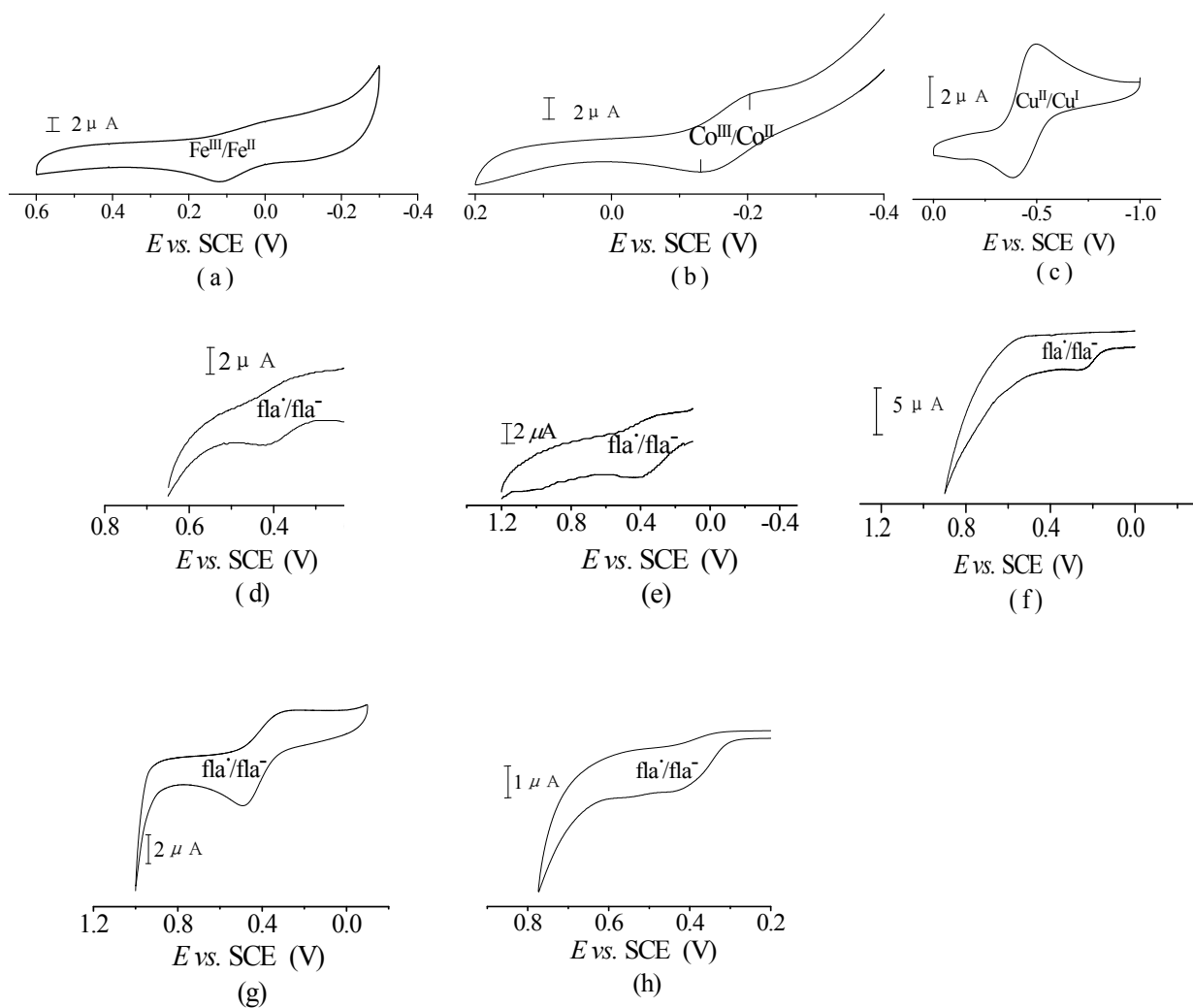


Figure S4. Cyclic voltammograms of (a) $[\text{Fe}^{\text{II}}\text{L}(\text{OAc})]$ (**2**), (b) $[\text{Co}^{\text{II}}\text{L}(\text{OAc})]$ (**3**), (c) $[\text{Cu}^{\text{II}}\text{L}(\text{OAc})]$ (**5**) and flavonol in the presence of 1 eq. (d) $[\text{Mn}^{\text{II}}\text{L}(\text{OAc})]$ (**1**), (e) $[\text{Co}^{\text{II}}\text{L}(\text{OAc})]$ (**3**), (f) $[\text{Ni}^{\text{II}}\text{L}(\text{OAc})]$ (**4**), (g) $[\text{Cu}^{\text{II}}\text{L}(\text{OAc})]$ (**5**) and (h) $[\text{Zn}^{\text{II}}\text{L}(\text{OAc})]$ (**6**) in DMF.

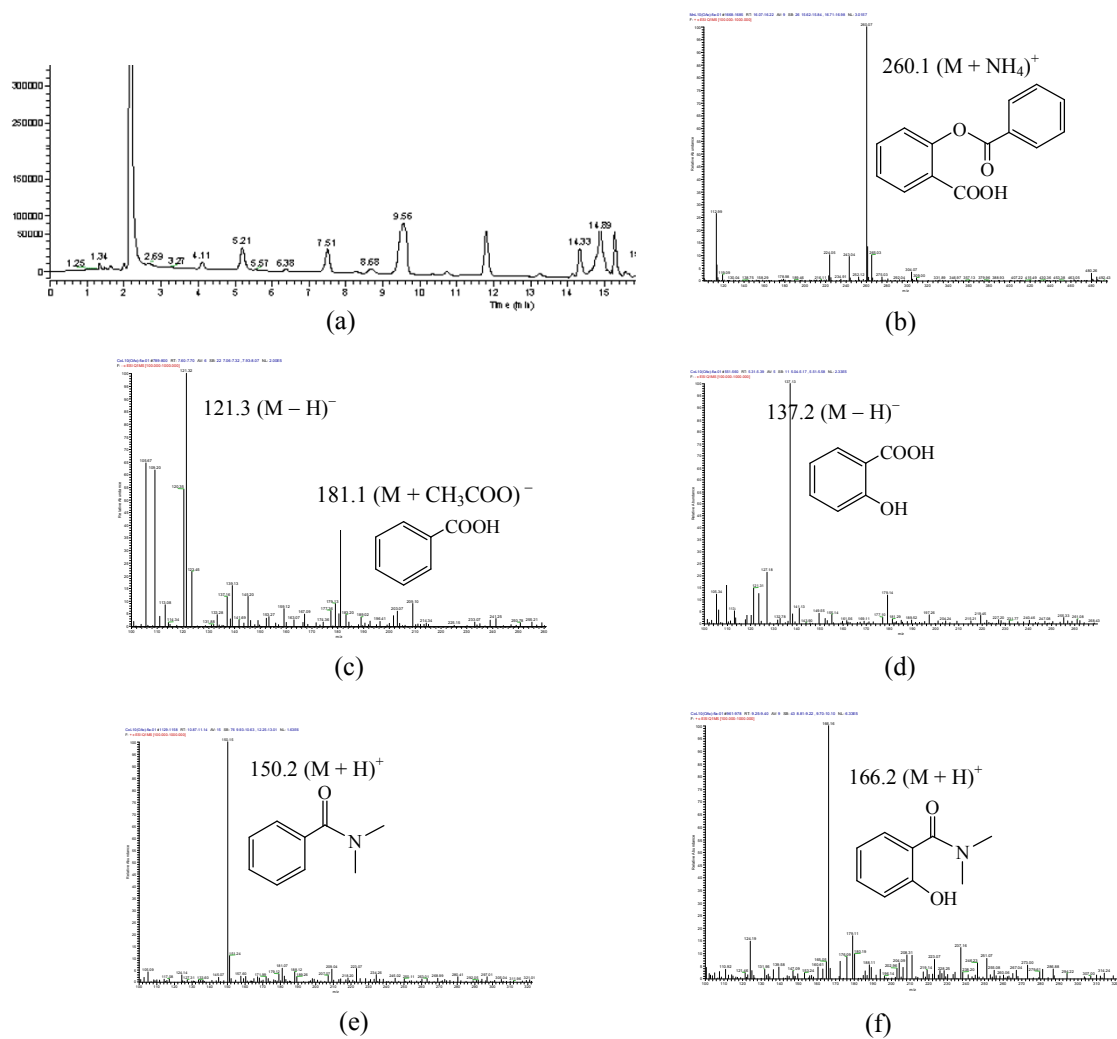


Figure S5. The HPLC-MS spectra of the reaction products of dioxygenation of flavonol catalyzed by $[\text{Co}^{\text{II}}\text{L}(\text{OAc})]$ (**3**) at 70°C for 12 hrs. (a) HPLC spectra. MS spectra of (b) HObs m/z (pos.): $260.1 (\text{M} + \text{NH}_4)^+$, (c) benzoic acid m/z (neg.): $121.3 (\text{M} - \text{H})^-$, $181.1 (\text{M} + \text{CH}_3\text{COO})^-$, (d) salicylic acid m/z (neg.): $137.2 (\text{M} - \text{H})^-$, (e) *N,N*-dimethylbenzamide m/z (pos.): $150.2 (\text{M} + \text{H})^+$ and (f) 2-hydroxy-*N,N*-dimethylbenzamide m/z (pos.): $166.2 (\text{M} + \text{H})^+$.

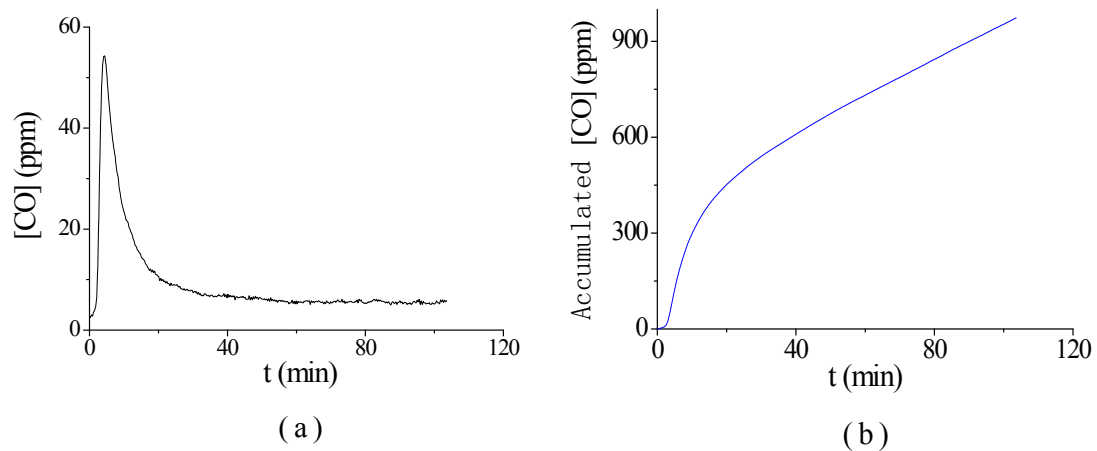


Figure S6. Detection of the production of CO during dioxxygenation reaction of flavonol catalyzed by $[\text{Co}^{\text{II}}\text{L}(\text{OAc})]$ (**3**) at 70 °C. (a) Plot of the CO concentration vs. reaction time. (b) Plot of the integrated CO concentration vs. reaction time.

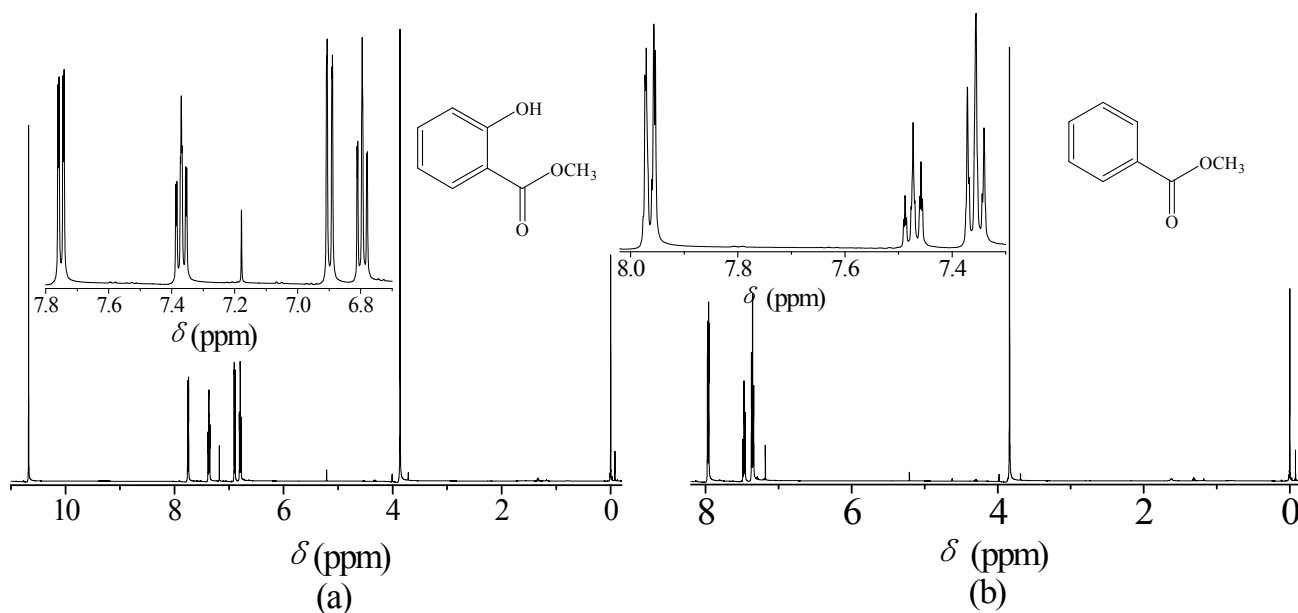


Figure S7. ^1H NMR spectra of two main products of reaction of flavonol (2.5×10^{-2} M in 200 mL DMF) with O_2 catalyzed by $[\text{Co}^{\text{II}}\text{L}(\text{OAc})]$ (**3**) (5% mol) at $100\text{ }^\circ\text{C}$ for 7 days after esterification by CH_3OH in the presence of H_2SO_4 at ambient temperature. (a) salicylic acid methyl ester (b) benzoic acid methyl ester.

Note: The ^1H NMR (CDCl_3 , 400 MHz) data of salicylic acid methyl ester and benzoic acid methyl ester. There are some solvent peaks in spectra.

Salicylic acid methyl ester: δ (ppm) 3.86 (s, 3 H, $-\text{COOCH}_3$), 6.80 (t, $J = 7.5$ Hz, 1 H, $\text{H}_{\text{Ph-5}}$), 6.90 (d, $J = 10$ Hz, 1 H, $\text{H}_{\text{Ph-3}}$), 7.37 (t, $J = 7.5$ Hz, 1 H, $\text{H}_{\text{Ph-4}}$), 7.75 (d, $J = 7.5$ Hz, 1 H, $\text{H}_{\text{Ph-6}}$), 10.68 (s, 1H, $-\text{OH}$).

Benzoic acid methyl ester: δ (ppm) 3.84 (s, 3 H, $-\text{COOCH}_3$), 7.36 (t, $J = 7.5$ Hz, 1 H, $\text{H}_{\text{Ph-4}}$), 7.47 (t, $J = 7.5$ Hz, 2 H, $\text{H}_{\text{Ph-3}}$, $\text{H}_{\text{Ph-5}}$), 7.96 (d, $J = 7.5$ Hz, 2 H, $\text{H}_{\text{Ph-2}}$, $\text{H}_{\text{Ph-6}}$).

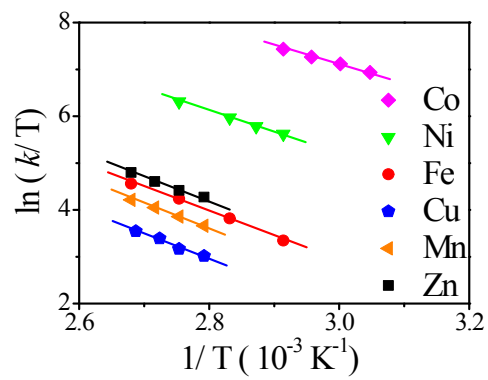


Figure S8. Eyring plot for the dioxygenation of flavonol catalyzed by the complexes $[\text{M}^{\text{II}}\text{L}(\text{OAc})]$ in DMF.

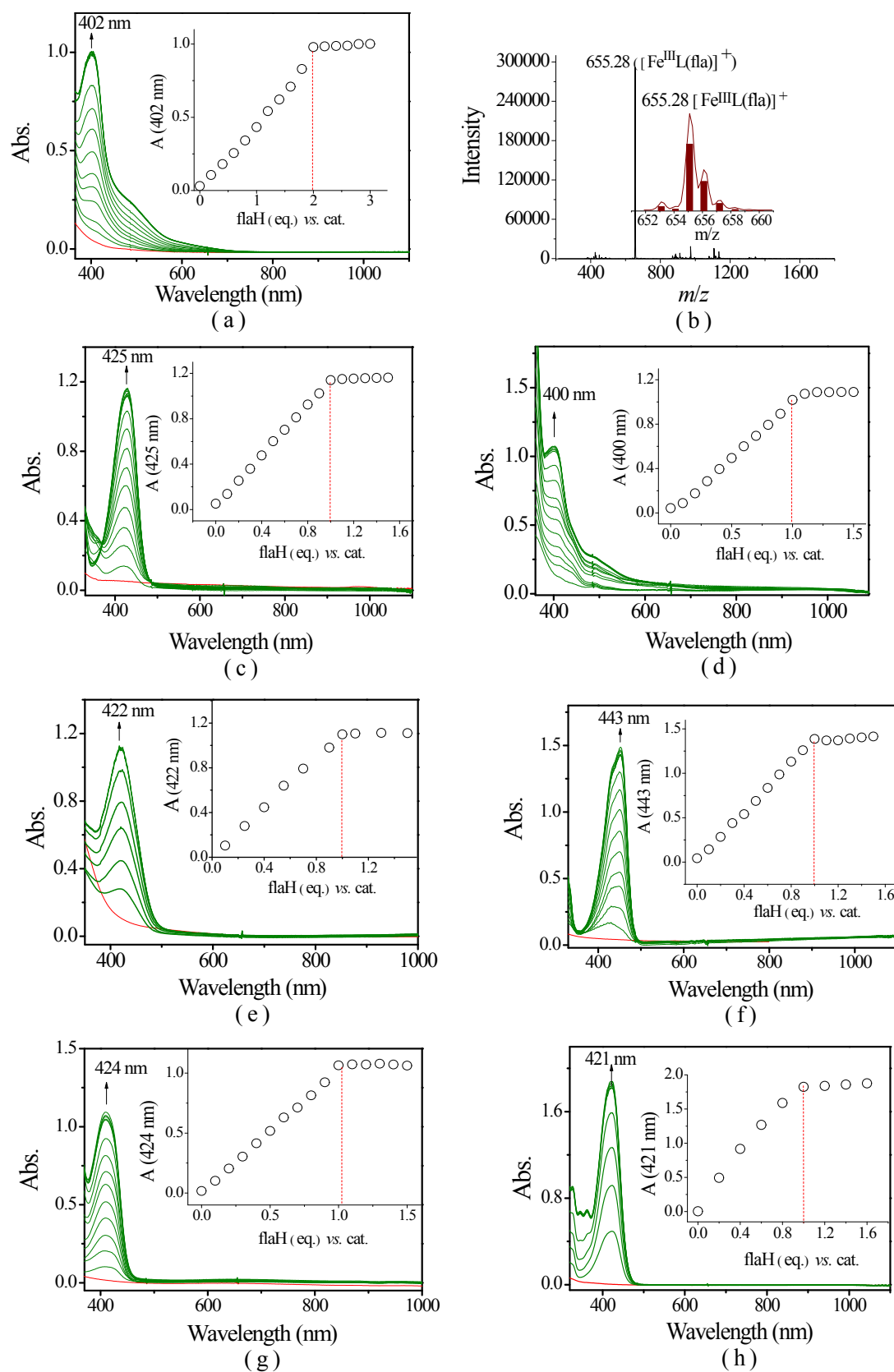


Figure S9. Spectral changes accompanying the titration of the complex (a) **2B**, (c) **1**, (d) **2**, (e) **3**, (f) **4**, (g) **5** and (h) **6** (1.0×10^{-4} M except **2B** 0.5×10^{-4} M) by flavonol under N_2 . Inset: Absorbance changes at λ_{\max} vs. eq. of flaH, (b) ESI-MS spectrum of the titration solution of **2B**.

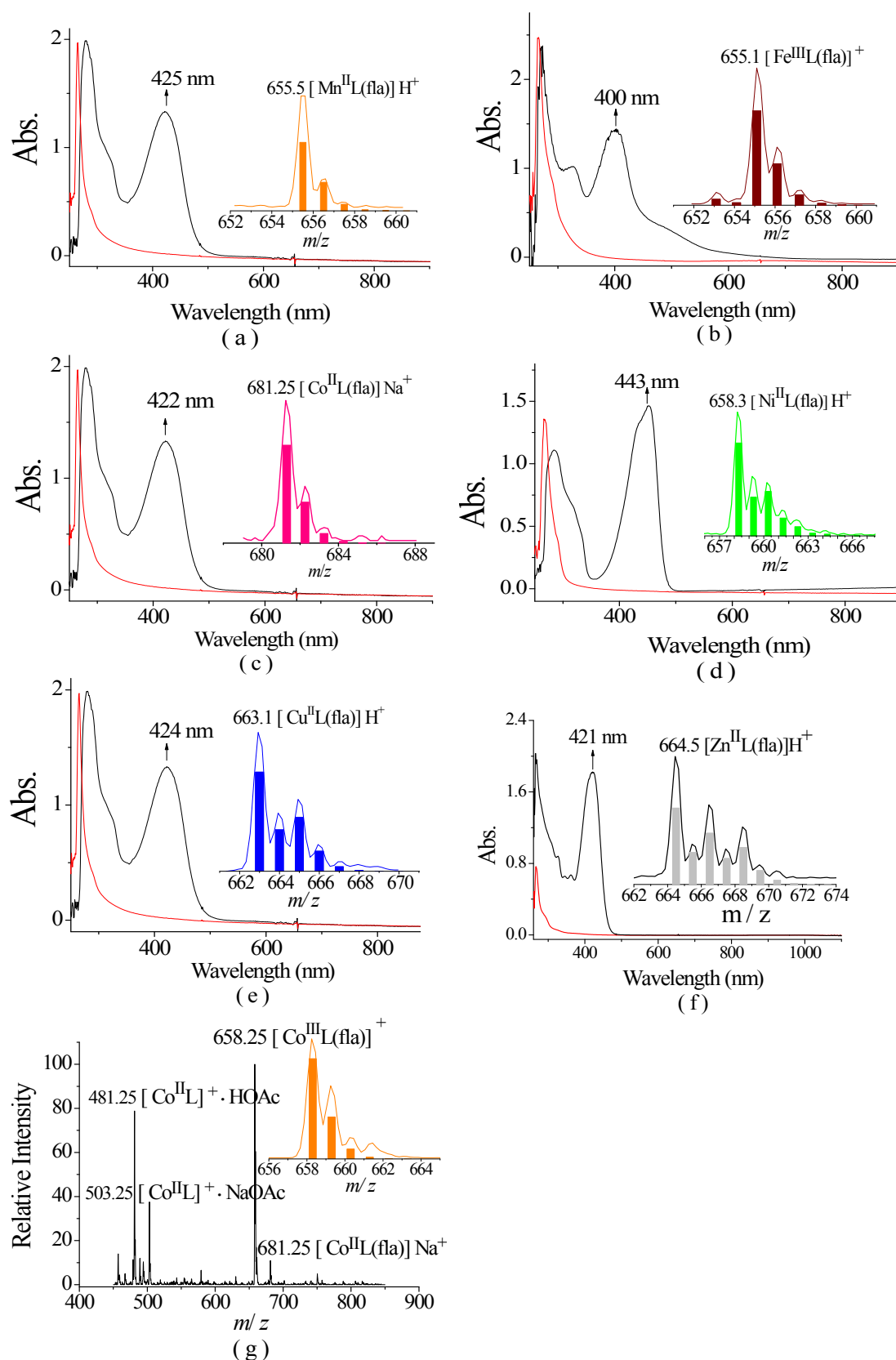


Figure S10. The UV-vis spectra of the complexes $[\text{M}^{\text{II}}\text{L}(\text{OAc})]$ (0.1 mM) (red) and in the presence of equivalent amount of flavonol (black) (a) $[\text{Mn}^{\text{II}}\text{L}(\text{OAc})]$ (**1**), (b) $[\text{Fe}^{\text{II}}\text{L}(\text{OAc})]$ (**2**), (c) $[\text{Co}^{\text{II}}\text{L}(\text{OAc})]$ (**3**), (d) $[\text{Ni}^{\text{II}}\text{L}(\text{OAc})]$ (**4**), (e) $[\text{Cu}^{\text{II}}\text{L}(\text{OAc})]$ (**5**), (f) $[\text{Zn}^{\text{II}}\text{L}(\text{OAc})]$ (**6**) (g) ESI-MS spectrum of the solution of $[\text{Co}^{\text{II}}\text{L}(\text{OAc})] + 1 \text{ eq. flaH}$ after exposure to O_2 . Inset: The peak cluster of $[\text{M}^{\text{II}}\text{L}(\text{fla})]\text{H}^+$ (M: Mn, Ni, Cu) or $[\text{M}^{\text{III}}\text{L}(\text{fla})]^+$ (M: Fe, Co) (Line: experiment, column: calculated).